ESC-TR-2006-073

Technical Report
1116

Advanced Narrowband Electromagnetic Size and Shape Determination

S. Kusiak

15 February 2008

Lincoln Laboratory
MASSACHUSETTS INSTITUTE OF TECHNOLOGY
LEXINGTON, MASSACHUSETTS

Prepared for the Department of the Army under Contract FA8721-05-C-0002.

This report is based on studies performed at Lincoln Laboratory, a center for research operated by Massachusetts Institute of Technology. This work was sponsored by the Department of the Army, under Air Force Contract FA8721-05-C-0002.

The ESC Public Affairs Office has reviewed this report, and it is releasable to the National Technical Information Service, where it will be available to the general public, including foreign nationals.

This technical report has been reviewed and is approved for publication.

FOR THE COMMANDER

Gary Tutungian
Administrative Contracting Officer
Plans and Programs Directorate
Contracted Support Management

Massachusetts Institute of Technology
Lincoln Laboratory

Advanced Narrowband Electromagnetic Size and Shape Determination

S. Kusiak
Formerly of Group 32

Technical Report 1116

15 February 2008

Lexington Massachusetts

ABSTRACT

We discuss a fundamental radar imaging problem for narrowband electromagnetic waves that extends the recent results originally obtained in [1, 2] in the scalar, or acoustic, setting. In particular we demonstrate the ability to efficiently image three-dimensional convex conducting bodies by using the knowledge of the scattered electric field for one fixed monochromatic illumination of the target. In this problem our knowledge of the scattered electric wave is understood to be in the form of measurements of the amplitude and phase of the tangential components of the radiated electric field (generated by the radar target) on a finite two-dimensional array. We also provide a more general version of this streamlined result that describes imaging of multiply connected nonconvex objects with the same measurements.

ACKNOWLEDGMENTS

The author would like to acknowledge and thank Dr. Keh-Ping Dunn (MIT LL) and Thang Lai (ADAC) for their support and sponsorship of this work.

TABLE OF CONTENTS

LIST OF ILLUSTRATIONS

1. INTRODUCTION

We begin with a few introductory remarks that outline what we mean by narrowband electromagnetic imaging. The problem concerns estimating the shape and size of an object on the basis of known information in the form of measurements of reflected waves taken at some distance from the unknown object. Specifically, how do we form a three-dimensional image of a potentially very distant object using something like a radar or collection of such sensors? Figure 1 depicts such a measurement scenario.

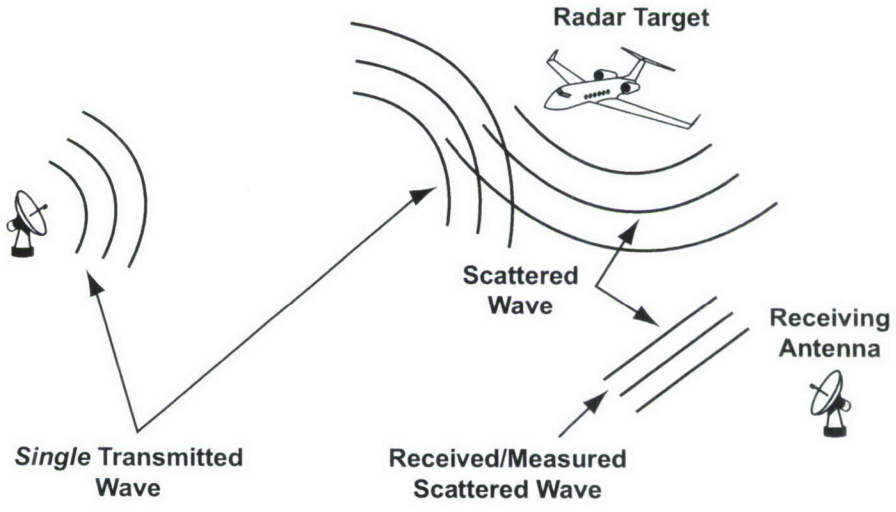

Figure 1. Data collection scenario.

The problem is simple: image the scatterer, or target, with a single incident wave with the aid of measurements of the scattered wave taken on a finite two-dimensional array. For example, the scattered wave is a frequency-dependent, i.e., narrowband, induced voltage response created by the illumination of the target. Although the underlying physics and mathematics that lead us to the imaging algorithm can appear complicated, the algorithm we will ultimately employ is extremely easy to understand and implement.

The imaging algorithm may be summarized as follows. The measured electric field, as a function of two variables on the array and for a chosen origin of the problem, is decomposed into its generalized Fourier modes, and a combined one-dimensional power spectrum of this signal is generated. The critical

point in the power spectrum where the combined spectral energy transitions from a highly oscillatory behavior and begins a super exponential decay is then found. This index is determined by computing the l^2 norm[1] of the accumulated energy of these modes and defining the cutoff at ninety percent of the total spectral energy. The index cutoff is converted to a length through division by the wave number ($2\pi/\lambda$) of the narrowband waveform used in probing the target. This length represents the radius of the smallest sphere, centered at the origin we previously specified, which must contain the unknown scatterer. The process is then repeated with new center, or origin, and terminated when enough centers of interest have been considered. Finally, the intersection of all the computed spheres is computed and the resulting common region is taken as an approximation to the convex scatterer.

We mention that the power spectrum possesses three very pronounced and particular behavior regimes as a function of increasing mode number. Figure 2 illustrates the three regions of interest and shows the combined power spectra, labeled as $|\beta_n|$ for a candidate example. The first regimes takes place within $0 \leq n \leq 45$, the second roughly within $45 \leq n \leq 55$, and the final region for all n beyond this.

1. i.e., L^2 norm of a discrete collection of complex numbers.

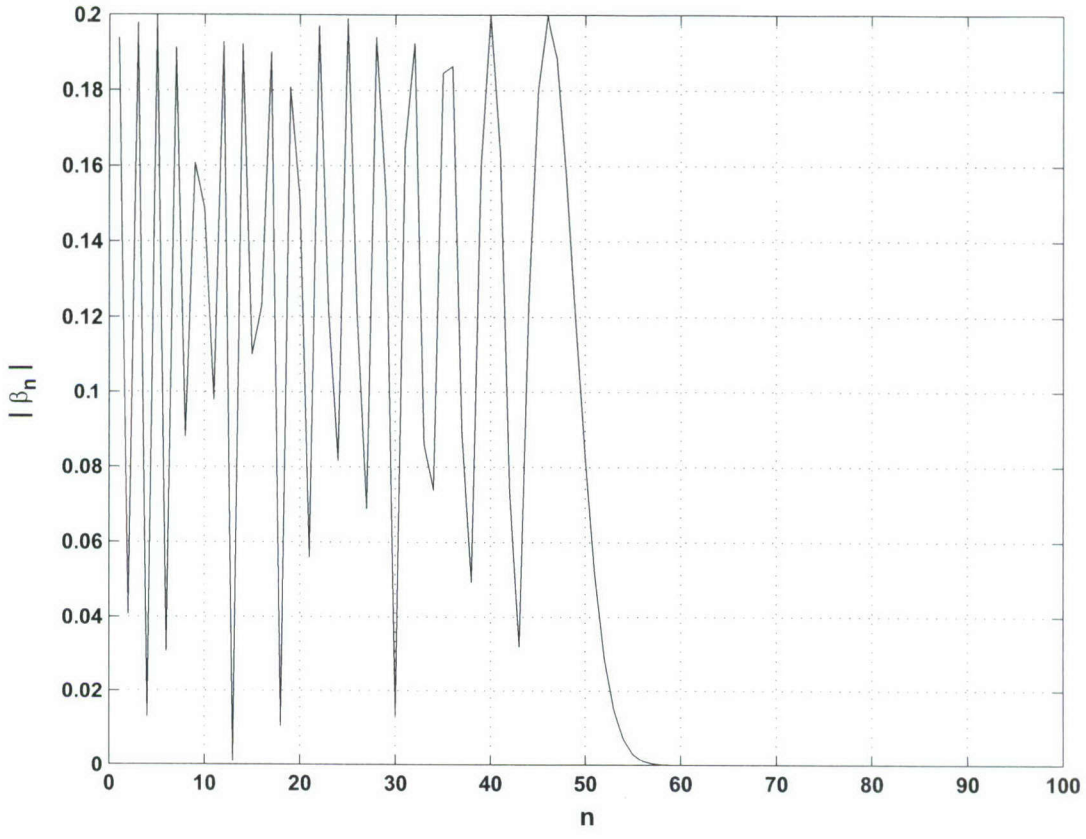

Figure 2. Oscillation and decay of the combined power spectra.

First, there is a region of highly oscillatory modes, followed by a region of extremely rapid decay, finally followed by a region of essentially null values. The index at which this power spectrum begins this rapid decline defines the radius of the smallest sphere with a specified origin, which must contain the scattering object.[2] By considering several origins we construct several such spheres, each of which must contain the scatterer. Hence, by considering the intersection of all such spherical regions we arrive at an approximation to a three-dimensional image of the assumed target. Figure 3 provides an illustration of this process.

---

2. For the moment, we mention that the reason for this is intimately related to the unique analytic continuation of the measured electric field on an array. We will revisit this in the section treating the supporting theory behind our main result and defer further discussion until such time, due to its technical nature.

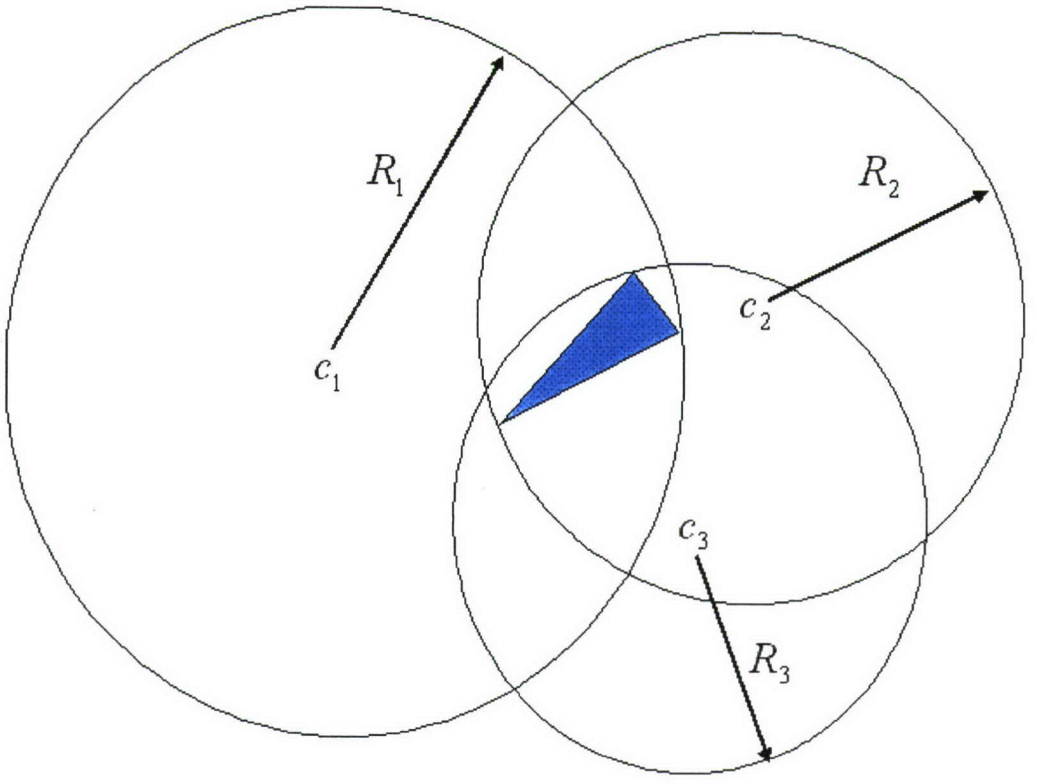

Figure 3. An example of two-dimensional projection of the intersection of three spherical-containing regions and the true convex target.

The remainder of this report reviews the physics that govern this problem and how that physics and some mathematical analysis lead to a well-understood and fully justified target characterization algorithm. Moreover, this treatment suggests additional innovative object characterization techniques through its description of the fundamental scattering processes at work. These results will be presented in forthcoming articles.

2. THE PHYSICAL MODEL

We begin with a brief overview of the fundamental inverse scattering problem at the heart of our application. Our imaging technique will employ novel processing of measurements of electromagnetic waves. Hence, to illustrate the origins, success, and limitations of the algorithm, we begin with a brief review and characterization of what we term the forward, or direct, scattering problem: given a well-defined scattering object and a specified incident wave, we formulate the response to that incident illumination and analytically predict how such a wave would interact with the scatterer.

We start with the time-dependent Maxwell's equations in free space, i.e., in a subdomain of $\Omega \subset R^3$ in which there are no electric or magnetic current densities, for which the electric field $\mathcal{E}$ and the magnetic field B satisfy

$$\nabla \wedge \mathcal{E}(x, t) + \mu_0 \partial_t B(x, t) = 0, \tag{1}$$

$$\nabla \wedge B(x, t) - \varepsilon_0 \partial_t \mathcal{E}(x, t) = 0. \tag{2}$$

Here, $x = (x_1, x_2, x_3) \in R^3$ is our spatial variable and $t \in R$ denotes time. The constant quantities μ_0 and ε_0 are, respectively, the magnetic permeability and electric permittivity of free space. We briefly mention that the electric and magnetic fields are complex-valued vector quantities as functions of both position and time, so that $\mathcal{E}$, B: $R^3 \times R \rightarrow C^3$. Additionally, $\nabla \wedge$ is the standard curl operation and ∂_t denotes differentiation in time.

Rather than dealing directly with the problem in the time domain, we will recast this system of six coupled partial differential equations into one that depends on frequency. On the basis of this system, we arrive at our narrowband, or fixed-frequency, imaging result.

To accomplish this goal, we employ the Fourier transform mapping functions, or distributions, in time into ones depending on angular frequency w. In this way we define frequency-dependent electric and magnetic fields as

$$E(x, w) = \int_R e^{-iwt} \mathcal{E}(x, t) dt \text{ and } H(x, w) = \int_R e^{-iwt} B(x, t) dt, \tag{3}$$

whose inversions are given by

$$\mathcal{E}(x,t) = \frac{1}{2\pi}\int_R e^{iwt}E(x,w)dw \quad \text{and} \quad B(x,t) = \frac{1}{2\pi}\int_R e^{-iwt}H(x,w)dw\,. \tag{4}$$

We note that $i = \sqrt{-1}$ represents the imaginary unit.

Employing the Fourier transform essentially converts differentiation in time into multiplication in frequency. Hence, we arrive at the frequency-dependent Maxwell system

$$\nabla \wedge E(x,w) - iw\mu_0 H(x,w) = 0\,, \tag{5}$$

$$\nabla \wedge H(x,w) + iw\varepsilon_0 E(x,w) = 0\,. \tag{6}$$

We now take a moment to distinguish between two fundamentally different types of electric and magnetic fields. By this we mean outgoing, or scattered or radiating waves (E^s, H^s), and incoming, or local incident plane waves (E^i, H^i). We define the total fields we would measure with any physical device as the sum of these two types of waves. Namely, we will use, and so we define here, the total fields E and H as

$$E(x) = E^i(x) + E^s(x), \qquad H(x) = H^i(x) + H^s(x)\,. \tag{7}$$

Any outgoing pair of electric and magnetic fields must satisfy the so-called Silver-Müller radiation condition, which we recall is given by either

$$\lim_{r\to\infty}(H^s \wedge x - rE^s) = 0, \qquad r = |x| \tag{8}$$

or

$$\lim_{r\to\infty}(E^s \wedge x + rH^s) = 0, \qquad r = |x|\,. \tag{9}$$

Equivalently, $E^s = (E_1^s, E_2^s, E_3^s)$ and $H^s = (H_1^s, H_2^s, H_3^s)$ means that each Cartesian coordinate component $E_j^s : R^3 \to C$ and $H_j^s : R^3 \to C, j = 1, 2, 3$, of the two vector fields E^s and H^s satisfies the Sommerfeld radiation condition, which is

$$\lim_{r \to \infty} (\partial_r - ik) E_j = \lim_{r \to \infty} (\partial_r ik) H_j = 0, r = |x| . \tag{10}$$

The Silver-Müller and Sommerfeld radiation conditions imply the asymptotic behaviors

$$E^s(x) = \frac{e^{ik|x|}}{|x|} (E_\infty(\hat{x}) + O(|x|^{-1})), \qquad |x| \to \infty , \tag{11}$$

and

$$H^s(x) = \frac{e^{ik|x|}}{|x|} (H_\infty(\hat{x}) + O(|x|^{-1})), \qquad |x| \to \infty , \tag{12}$$

where $\hat{x} = (x/|x|)$ and $|x|^2 = x_1^2 + x_2^2 + x_3^2$. Here, the quantities E_∞ and H_∞ denote the far-field patterns, or scattering amplitudes, of the outgoing waves $E^s(x)$ and $H^s(x)$. We emphasize that for most remote electromagnetic sensing experiments, these are the quantities we measure. Additionally, the electric and magnetic scattering amplitudes defined on the unit sphere with normal v_{s^2} must also satisfy the asymptotic boundary conditions

$$\langle v_{s^2}, E_\infty \rangle = \langle v_{s^2}, H_\infty \rangle = 0, \quad \text{where } H_\infty = v_{s^2} \wedge E_\infty . \tag{13}$$

We mention that this equation simply means that the electric and magnetic scattering amplitudes are purely tangential vector fields, possessing no normal contribution in any direction $\hat{x} \in S^2$.

Incoming electric and magnetic waves are ones similar to the radiating case, only they satisfy the conjugate of the Silver-Müller and Sommerfeld radiation conditions. That is, rather than having constant phase fronts that migrate outward, in the usual sense, they travel and converge on the origin as a function of positive time. Additionally, by a local plane wave propagating in the direction $\hat{y}$ we mean a certain type of incoming wave—specifically, a Herglotz wave with a Dirac kernel supported in the direction $\hat{y}$.

We will now turn our attention to the case of the scattering of an incident wave pair (E^i, H^i) from a perfect conducting scatterer. In particular, what we mean is that the tangential components of the total electric field must vanish throughout the surface of the scatterer, so that if $v_D(x)$ denotes this normal of the scatterer D at some point x, then we have

$$\nu_D(x) \wedge E(x) = 0, \qquad \forall x \in \partial D. \tag{14}$$

In summary, the problem is to understand how an incident pair of fields (E^i, H^i) interacts with the conductor D and generates the scattered pair of fields (E^s, H^s) as a function of various parametrizations of the incident wave energy, e.g., their frequency or energy and direction. We note that the problem may be stated and treated as a system of partial differential equations, admitting very insightful analysis and solution techniques via the theory of finite elements. For more on this approach see [3, 4]. For the purposes of the exposition of this report, however, we will choose to frame this problem in terms of integral equations for the clarity they provide in terms of the operator mappings between the scattering system inputs (E^i, H^i) and its outputs (E^s, H^s).

In any domain $\Omega \subset R^3$ within which there are no charge or current sources, each type of outgoing or incoming wave satisfies our frequency-dependent Maxwell system

$$\nabla \wedge E^{i,s} - ikH^{i,s} = \nabla \wedge H^{i,s} + ikE^{i,s} = 0, \qquad k = w/c = w(\mu_0 \varepsilon_0)^{-1}, \tag{15}$$

and hence, the total fields E and H do as well. This system of coupled partial differential equations has an alternative integral equation representation called the Stratton-Chu integral equation, which for a perfect conductor has the form

$$E(x) = E^i(x) + \frac{i}{k}\nabla \wedge \nabla \wedge \int_{\partial D} G(x-y)\nu(y) \wedge H(y)ds(y), \tag{16}$$

$$H(x) = H^i(x) + \nabla \wedge \int_{\partial D} G(x-y)\nu(y) \wedge H(y)ds(y). \tag{17}$$

Here, $ds(y)$ denotes surface measure on the boundary of the conducting scatterer D, and the integrals exist as improper ones as $x \to \partial D \ni y$. Again, we emphasize that the pair (E, H) denotes the total electromagnetic and magnetic fields, and we identify the integral kernel $G(x-y)$ appearing in both integral equations as the fundamental solution of the scalar Helmholtz equation. Specifically, G is the outgoing fundamental, or distributional, solution of

$$(\Delta + k^2)G(x-y) = \delta(x-y), \quad x, y \in R^3, \quad \Delta = \sum_{j=1}^{3} \partial_{x_j^2}, \tag{18}$$

where $\delta \in \mathcal{E}'(R^3)$ is the so-called Dirac distribution, or "delta function," and is given by

$$G(x-y) = \frac{1}{4\pi}\frac{e^{ik|x-y|}}{|x-y|}, \qquad x \neq y. \tag{19}$$

The asymptotic behavior of the convolution kernel G is of extreme importance; hence, we take a few moments to examine it. Suppose the point y is contained within the finite ball of radius R centered at the origin, which we write as $B_R(0)$. Suppose further that $\hat{x} = x/|x| \in S^2 = \{x \in R^3 : x_1^2 + x_2^2 + x_3^2 = 1\}$ and $G(x)$ is the outgoing fundamental solution to the operator $\Delta + k^2$ in R^3. Then,

$$G(x-y) \sim \frac{1}{4\pi}\frac{e^{ik|x|}}{|x|}e^{-ik\langle \hat{x}, y\rangle}, \qquad x \to \infty. \tag{20}$$

This claim is evident when we examine the asymptotics of the term $|x-y|$. First, if y is required to remain in a finite region, while x may tend to infinity, then

$$|x-y| = |x| + \frac{\langle \hat{x}, y\rangle}{|x|} + O(|x|^{-2}), \qquad |x| \to \infty. \tag{21}$$

Since $y \in B_R(0)$, then

$$\max_{\hat{x} \in S^2} |\langle \hat{x}, y\rangle| \leq R < \infty. \tag{22}$$

Hence,

$$G(x-y) = \frac{1}{4\pi}\frac{e^{ik|x|}}{|x|}e^{-ik\langle \hat{x}, y\rangle}(1 + O(|x|^{-1})), \qquad |x| \to \infty. \tag{23}$$

The asymptotic behavior of the acoustic outgoing fundamental solution G coupled with the asymptotic behavior of the scattered electric and magnetic waves implies that the electric and magnetic scattering amplitudes are given by

$$E_\infty(\hat{x}) = \frac{ik}{4\pi}\hat{x} \wedge \int_{\partial D} e^{-ik\langle \hat{x}, y\rangle} \nu((y) \wedge H(y)) \wedge \hat{x} ds(y) \tag{24}$$

$$H_\infty(\hat{x}) = \frac{ik}{4\pi}\hat{x} \wedge \int_{\partial D} e^{-ik\langle \hat{x}, y\rangle} \nu((y) \wedge E(y))ds(y)\,. \tag{25}$$

The formulations for the electric and magnetic scattering amplitudes now provide us an operator we term F, whose analytical properties will be of significant interest. It tells how and why we can image conducting bodies with narrowband measurements of the scattered electromagnetic waves made at a distance. For this reason we will examine a few more aspects of the operator F and briefly discuss how it indicates and describes the interaction between an incident incoming magnetic wave H^i and a conducting body. More importantly, we will hit on how such a description benefits us in suggesting a reconstruction, or three-dimensional imaging algorithm.

From the previous analysis we see that the electric scattering amplitude is generated by the surficial current $j = \nu_D \wedge H$ generated on the boundary of the conductor D by the interaction of an incident pair of waves (E^i, H^i). In summary,

$$E_\infty(\hat{x}) = (Fj)(\hat{x}) := \int_{\partial D} K(\hat{x}, y)j(y)ds(y)\,, \tag{26}$$

where the kernel of operator F is

$$K(\hat{x}, y) := -\frac{ik}{4\pi} e^{-ik\langle \hat{x}, y\rangle} \hat{x} \wedge \hat{x} \wedge. \tag{27}$$

If we recall and write the second of the Stratton-Chu integral equations as a function of the incident magnetic wave

$$H^i_\alpha = \int_{S^2} e^{ik\langle y, \hat{x}\rangle} \alpha(\hat{x})ds(\hat{x}), \qquad \alpha \in TL^2(S^2)\,, \tag{28}$$

where the subscript indicates the parametrization of H^i—e.g., in this instance H^i_α is a superposition of entire plane waves, also called Herglotz waves, and plays the role of the weighting of such square integrable tangential vector waves and is the Herglotz kernel—as

$$H(x) = H^i_\alpha(x) + \nabla \wedge \int_{\partial D} G(x - y)\nu(y) \wedge H(y)ds(y) \tag{29}$$

$$=: H^i(x) + (BH)(x)\,, \tag{30}$$

then, formally given an known parametrization of an incident magnetic wave H^i_α, the electric scattering amplitude is generated by

$$E_\infty(\hat{x}) = \int_{\partial D} K(\hat{x}, y) \nu_D \wedge ((I - B)^{-1} H^i_\alpha)(y) ds(y) \tag{31}$$

$$=: (\tilde{\mathrm{F}} H^i_\alpha)(\hat{x}), \qquad \hat{x} \in A\,. \tag{32}$$

In the next section, we present the main result of this report, which is that the coefficients in the generalized Fourier series representation of E_∞ on A encode the boundary of the scatterer ∂D. Moreover, this result gives us a robust and efficient algorithm that can reconstruct the scatterer with limited but appropriately sampled values of E_∞ on A. The details of the properties of F and the representation of the signal E_∞ on the array A that support these results will then be discussed in detail in Section 4.

3. MAIN RESULTS

Before discussing the main results we need to address two issues. The first concerns the dependence of the electric scattering amplitude on the origin of the physical problem. Since we are at liberty to define the origin where we choose and this value changes the values of the measured quantity we have, we must determine this influence. Moreover, we will demonstrate that this analysis leads us to a very attractive and easily implementable algorithm for characterizing the scattering body. The second issue regards the vector representation of the tangential vector field on our measurement array.

We begin with a quick treatment of the continuous dependence of the electric scattering amplitude with the origin $c \in R^3$. In what we developed in the previous section, we assumed the origin to be the standard one, namely, $c = 0$. However, if instead we choose any arbitrary point c to be the center of our universe, then the electric scattering amplitude is generated by

$$E_\infty(\hat{x}) = (Fj(-c))(\hat{x}) \tag{33}$$

$$= \int_{\partial D - c} K(\hat{x}, y) j(y - c) ds(y) \tag{34}$$

$$= -\frac{ik}{4\pi} \int_{\partial D - c} e^{-ik\langle \hat{x}, y\rangle} \hat{x} \wedge \hat{x} \wedge j(y - c) ds(y) \tag{35}$$

$$= -\frac{ik}{4\pi} e^{ik\langle \hat{x}, c\rangle} \int_{\partial D} e^{-ik\langle \hat{x}, y\rangle} \hat{x} \wedge \hat{x} \wedge j(y) ds(y) \tag{36}$$

$$= \Phi_c(\hat{x})(Fj)(\hat{x}), \qquad \Phi_c(\hat{x}) = e^{ik\langle \hat{x}, c\rangle}, \tag{37}$$

where ∂D-c is the translate of ∂D to the c-centered origin. Hence, given the true scattering amplitude E_∞ produced by the physical interaction with the incident wave, we may produce its value if instead we insist that the point c is the origin by performing a unitary operation, i.e., a simple phase multiplication at each point where we measure the field. We further add that this concept of shifting and choosing various origins plays a very powerful and useful role in the imaging algorithm.

We recall that the electric scattering amplitude we measure in remote sensing on a flat or curved two-dimensional array will consist of two orthogonal components. By this we mean that the electric scattering

amplitude is a vector-valued function. Also, since any flat or smoothly curved array is locally equivalent to the unit sphere, we begin with a very brief discussion of two-dimensional vector fields supported on the unit sphere S^2. In what follows, for a scalar function $u(\theta, \phi)$ defined on the unit sphere S^2, we will use the so-called surficial gradient, defined by

$$\nabla_{S^2} u = \left(\frac{1}{\sin\theta} \frac{\partial u}{\partial \phi}, \frac{\partial u}{\partial \theta} \right), \tag{38}$$

which is an element of the tangent space of the unit sphere, denoted by T_{S^2}.

Let v be a complex-valued vector field supported on the unit sphere S^2. Then we say that $v \in TL^2(S^2)$, provided that in the representation of the vector field on the sphere S^2

$$v(\hat{x}) = \sum_{n=1}^{\infty} \sum_{m=-n}^{n} \alpha_n^m \nabla_{S^2} Y_n^m(\hat{x}) + \beta_n^m x \wedge \nabla_{S^2} Y_n^m(\hat{x}), \qquad \hat{x} \in S^2 , \tag{39}$$

obeys the condition

$$\int_{S^2} \left(\left| \langle v(\hat{x}), \nabla_{S^2} \overline{Y_n^m(\hat{x})} \rangle \right|^2 + \left| \langle v(\hat{x}), \hat{x} \wedge \nabla_{S^2} \overline{Y_n^m(\hat{x})} \rangle \right|^2 \right) ds(\hat{x}) < \infty , \tag{40}$$

where the terms $\langle v, \nabla_{S^2} \overline{Y_n^m} \rangle$ and $\langle v, \hat{x} \wedge \nabla_{S^2} \overline{Y_n^m} \rangle$ represent the projections of the tangential field on S^2 onto the orthonormal bases $\nabla_{S^2} Y_n^m$ and $\hat{x} \wedge \nabla_{S^2} Y_n^m$. Here, the functions $Y_n^m(\hat{x})$ are the spherical harmonics, of order n and degree m on S^2 with $\hat{x} = \sin\theta, \cos\phi, \sin\theta \sin\phi, \cos\theta$, $\theta \in [0, \pi]$ and $\phi \in [0, 2\pi]$. For our purposes we define the harmonic functions in the following way:

$$\begin{aligned} Y_n^m(\theta, \phi) :&= (-1)^m \sqrt{\frac{2n+1}{4\pi} \frac{(n-|m|)!}{(n+|m|)!}} P_n^m(\cos\theta) e^{im\phi} \\ &= \varepsilon_m \sqrt{\frac{2n+1}{4\pi} \frac{(n-m)!}{(n+m)!}} P_n^m(\cos\theta) e^{im\phi}, \qquad \varepsilon_m = \begin{cases} -1^m, & m \geq 0 \\ 1, & m \leq 0 \end{cases} \end{aligned} \tag{41}$$

Above, the functions $P_n^m(\cos\theta)$ are the associated Legendre functions; c.f. [5, 6] for more details on their various properties and governing equation. This definition of the spherical harmonics allows us to express their complex conjugates as simply

$$\overline{Y_n^m(\hat{x})} = Y_n^{-m}(\hat{x}). \tag{42}$$

Also, this definition yields a complete orthonormal set on $L^2(S^2)$ in the sense that

$$\int_{S^2} \overline{Y_n^m(\hat{x})} Y_{n'}^{m'}(\hat{x}) dS(\hat{x}) = \delta_{n,n'}^{m,m'}, \tag{43}$$

where $\delta_{n,n'}^{m,m'}$ is the Kronecker delta. Lastly, we note that the finiteness criterion amounts to requiring that the generalized Fourier coefficients satisfy

$$\sum_{n=1}^{\infty} \sum_{m=-n}^{n} \left|\alpha_n^m\right|^2 + \left|\beta_n^m\right|^2 < \infty. \tag{44}$$

We now have all the key ingredients in place and state the main result of this article as the following theorem.

Theorem 1. Let $B_R(c)$ denote the sphere of finite radius R centered at the point $c \in R^3$, and let E_∞ be known on some section $\Gamma \subset S^2$ of the unit sphere and have a series expansion in tangential spherical harmonics defined on Γ,

$$E_\infty(\hat{x}) = \sum_{n=1}^{\infty} \sum_{m=-n}^{n} \alpha_n^m \nabla_{S^2} Y_n^m(\hat{x}) + \beta_n^m \hat{x} \wedge \nabla S^2 Y_n^m(\hat{x}), \qquad \hat{x} \in \Gamma, \tag{45}$$

with Fourier coefficients depending on R and c. Then the following are equivalent

1. $B_R(c)$ contains ∂D
2. There exists a magnetic current j supported within $B_R(c)$, depending on R and c, such that

$$E_\infty(\hat{x}) = \int_{B_R(c)} K(\hat{x} - y) j(y) dy, \qquad \hat{x} \in \Gamma. \tag{46}$$

3. The weighted energy of the Fourier coefficients, depending on R and c, is finite.

$$\sum_{n=1}^{\infty} w_n(R,c) \sum_{m=-n}^{n} \left|\alpha_n^m(R,c)\right|^2 + \left|\beta_n^m(R,c)\right|^2, \qquad w_n(R,c) = \left(\frac{2n}{ek(R+|c|)}\right)^{2n}. \tag{47}$$

Remark 1. The theorem states several important facts all at once. In summary, each item implies one another, which is to say that given any item, the other two are true as well. In what follows we address these implications and provide some explanation.

To begin it states that if the scatterer ∂D can be placed or fully contained within some sphere of radius R centered at the point c, then there exists a magnetic current supported on the boundary of a two-dimensional surface contained within this sphere, which when integrated against the kernel of the electric scattering amplitude generator yields the known electric scattering amplitude E_∞.

Next, the result states that such a scattering amplitude must have partial Fourier coefficients that decay faster than $(2n/ek(R+|c|))^{2n}$, as n tends to infinity. This is the observable quantity we exploit for various centers c, which then determines the value of R for each such c. Upon intersecting all such spheres for an appropriate collection of centers, this quantity yields an approximation of the convex hull of the scatterer, which if the scatterer is convex is an approximation of the scatterer itself. We note that in the limit that $|c|$ tends to infinity and the approximations of the convex hull of ∂D become better and better, theoretically speaking. From a numerical point of view this approximation becomes more and more difficult, as it requires the computation of higher and higher Fourier modes, which is difficult due to the rapid oscillation of the spherical harmonics for large n. However, even numerically speaking, this approximation can still be done if we utilize arbitrary machine precision techniques.

Lastly, if what we call the weighted energy of the Fourier coefficients converges for some R and center c, then it must be that there exists a sphere with such a radius and center that contains the totality of the scatterer ∂D, which in turn implies that the electric scattering amplitude is generated by some magnetic current on the surface of some two-dimensional manifold contained within such a sphere.

In a sense, what is going on here has to do with the analytic continuation of an analytic function. The function E_∞ is analytic in several variables, $\hat{x}$ and k, for instance. Furthermore, it is analytic in x, which means if we know it on some distant surface away from the scatterer ∂D, the function may be analytically continued up to the boundary of the scatterer. Where this continuation is no longer possible coincides with R for any given c, and means that no longer will the weighted Fourier coefficients converge, and no longer is there a magnetic current that can be integrated over such a smaller sphere and give rise to the known field E_∞.

We now offer a concise version of this result in the form of an algorithm that has been successfully implemented in the acoustic setting.

Algorithm 1. (Convex 3D Imaging).

1. Measure E_∞ on some two-dimensional array A.

2. Determine the tangential analysis eigenfunctions spanning the array A that are used to determine the spectrum, i.e., generalized Fourier coefficients, of the signal E_∞ (functions such as ∇Y_n^m and $\hat{x} \wedge \nabla Y_n^m$ in the case when A is the unit sphere[3]).

3. Optimally span a collection of points c and compute the associated generalized Fourier coefficients for that center.

4. Determine the radius R for each such center by examining where the partial sums of the Fourier coefficients begin a rapid transition to zero.

5. Intersect all such spheres to define the approximation of the convex hull of the scatterer.

Remark 2. We are also compelled to make another remark concerning the uniqueness of reconstructing the true scatterer in this problem. Our main result states that the measured asymptotic wave we know may be analytically continued in a unique fashion up to some natural boundary that corresponds to the boundary of some scatterer. To be fair, we must mention that in general this scatterer need not coincide with the true scatterer of interest. Rather, what we ultimately arrive at in this process is the so-called *scattering support* of the measured field, or the scatterer. See [1, 2] for more of the fundamental details concerning this object, as this object can be highly nontrivial and rather complex. For our purposes here, we define this object through the following convention.

Definition 1. Let ch(supp f) denote the convex hull of the support of a distribution f and let $s = -1/2$. Then the convex scattering support of the far field E_∞ for a perfectly conducting electromagnetic scatterer is

$$cS_k supp\ E_\infty = \bigcap_{Ff = E_\infty} ch(supp\ f), \tag{48}$$

where $f \in TL^2\left(\overset{o}{H}{}^S(R^3)\right)$.[4]

What we can uniquely determine is the common element to all candidate scattering objects that could give rise to the measured field of interest. We need to make this interjection and state this result, since to date there is no rigorous proof that a perfectly conducting scatterer may be uniquely determined

---

3. For more complex measurement arrays, these eigenfunctions may be analytically or numerically computed by treating a standard eigenvalue, eigenfunction problem whose formulation follows from the spectral theory of compact linear operators presented in the next section.

4. The space of distributions $\overset{o}{H}{}^S(R^3)$ for $s = -1/2$ is the standard Sobolev space $H^{-1/2}(R^3)$ of distributions having compact support in R^3; i.e., they are TL^2 vector fields on a two-dimensional manifold such as the surface of a sphere. Moreover, since we are assuming that the scatterer is perfectly conducting, we may specify $s = -1/2$ rather than having to take more general values of s falling within the interval $(-2, 0)$ for which the original theory of scattering support was developed.

from one single fixed energy excitation with measurements taken on such a section of the unit sphere, or two-dimensional array. Nonetheless, on the basis of uniqueness results and several numerical studies of this problem in the acoustic setting, it is widely suspected that the convex scattering support and the scatterer's true support are one and the same in the case of a perfectly conducting electromagnetic obstacle. A careful study and proof of this conjecture would constitute a major breakthrough in the academic realm of scattering theory; however, it is beyond the current scope of this report.

Remark 3. We should also take a moment to offer a generalization of this result, which allows us to image more complex three-dimensional targets that need not be convex. In the case of multiply connected nonconvex targets, we can offer a theoretically based method that can image such systems. However, a practical numerical implementation of such a result has yet to be done and is beyond the work presented in [7].

More generally, we have the following formulation.

Theorem 2. If Ω denotes a (possibly) multiply connected finite subset of R^3, and E_∞ is known on some section $\Gamma \subset S^2$ of the unit sphere and has a series expansion in tangential spherical harmonics defined on Γ,

$$E_\infty(\hat{x}) = \sum_{n=1}^{\infty} \sum_{m=-n}^{n} \alpha_n^m \nabla_{S^2} Y_n^m(\hat{x}) + \beta_n^m \hat{x} \wedge \nabla_{S^2} Y_n^m(\hat{x}), \qquad \hat{x} \in \Gamma, \tag{49}$$

with Fourier coefficients depending on Ω then, the following are equivalent:

1. Ω contains ∂D.
2. There exists a magnetic current j, supported within and depending on Ω, such that

$$E_\infty(\hat{x}) = \int_\Omega K(\hat{x} - y) j(y) dy, \qquad \hat{x} \in \Gamma. \tag{50}$$

3. The weighted energy of the Fourier coefficients, now depending on Ω, is finite.

$$\sum_{n=1}^{\infty} w_n(\Omega) \sum_{m=-n}^{n} \left|\alpha_n^m(\Omega)\right|^2 + \left|\beta_n^m(\Omega)\right|^2 . \tag{51}$$

For the purpose of brevity we shall not go into the rather complex nature of the exact asymptotics of these more generalized weights $w_n(\Omega)$, since their description is so highly connected with the geometry and number of components of Ω. We shall have to content ourselves that this formulation extends the previous theorem and represents the more general methodology of imaging nonconvex scatterers, since the test region Ω is allowed to be nonconvex, whereas the aforementioned spheres were not.

In the supporting theory to follow in the next section we give the appropriate indications that corroborate the claim made here and tie it to a result previously obtained in the scalar acoustic scattering case [7]. Additionally, we provide the mathematical machinery that yields a numerically feasible algorithm that can image such scatterers of interest.

4. SUPPORTING THEORY

We begin with a basic physical treatment of the scattering problem that inspires the more rigorous supporting theory, which underpins the two theorems given in the previous section.

The scattering of a fixed monochromatic electromagnetic wave of wave number $k = 2\pi/\lambda$ from a perfect conductor ∂D situated in the ball $B_R(0)$ is equivalent to the radiation problem

$$\nabla \wedge E^s(x) - ikH^s(x) = \nabla \wedge H^s(x) + ikE^s(x) = 0, \qquad x \in R^3 \backslash (\partial D \cap D), \tag{52}$$

where

$$E^s\big|_{\partial D} = v \in TL^2(\partial D) \tag{53}$$

is specified. The general solution of such a radiation problem in the complement of $B_R(0)$ admits the form

$$E^s(x) = \sum_{n=1}^{\infty} \sum_{m=-n}^{n} \alpha_n^m \nabla \wedge (x h_n^{(1)}(kr) Y_n^m(\hat{x})) + \beta_n^m \nabla \wedge \nabla \wedge (x h_n^{(1)}(kr) Y_n^m(\hat{x})), \qquad r = |x| > R, \tag{54}$$

where $h_n^{(1)}$ is the spherical Hankel function of the first kind—c.f. [6]—and is defined by

$$h_n^{(1)}(z) = j_n(z) + iy_n(z) , \tag{55}$$

with j_n and y_n respectively denoting the standard spherical Bessel functions of the first and second kind.

Examining the asymptotic behavior of the outgoing electric field leads to the electric scattering amplitude, which is known to have the form [8]

$$E_\infty(\hat{x}) = \frac{1}{k} \sum_{m=-n}^{n} i^{-1-n} k \beta_n^m \nabla_{S^2} Y_n^m(\hat{x}) - \alpha_n^m v_{S^2} Y_n^m(\hat{x}) . \tag{56}$$

Moreover, the tangential electric scattering amplitude is an element of $TL^2(S^2)$ only if

$$\sum_{n=1}^{\infty} \left(\frac{2n}{ekR}\right)^{2n} \sum_{m=-n}^{n} \left|\alpha_n^m\right|^2 + \left|\beta_n^m\right|^2 < \infty, \qquad \forall R > \operatorname{diam}(\partial D) . \tag{57}$$

The necessity of the weighted summability of the Fourier coefficients α_n^m and β_n^m is a consequence of the asymptotic behavior of the spherical Hankel functions as a function of its index n. For a fixed positive argument z,

$$h_n^{(1)}(z) \sim \left(\frac{2n}{ekz}\right)^n, \qquad n \to \infty . \tag{58}$$

Hence, E^s has a finite L^2 norm on the surface of any sphere of radius $r > R$ in $TL^2(B_r(0))$ only if the partial sum of the combined Fourier coefficients decay faster than $\left|h_n^{(1)}(|z|)\right|^2$ as $n \to \infty$ for all $r > |z|$. For each such r, where we see this convergent behavior indicates where the radiation problem may be posed as a homogeneous Maxwell system, i.e., how far in toward the origin the analytic scattered field may be uniquely continued as a free solution to the Maxwell system. That value r^* where the analytic continuation may no longer be performed defines the boundary of the scatterer. The analysis to follow treats the operators involved in the scattering problem and formalizes this basic physical principle.

$$\sum_{m=-n}^{n} \left|\alpha_n^m\right|^2 + \left|\beta_n^m\right|^2 . \tag{59}$$

To begin this analysis, we note that we need know only the electric scattering amplitude on some sector, or neighborhood, of the unit sphere. The significance of this is that there exists a collection of coordinate charts $\{\varphi_j\}_1^N : R^2 \to S^2$ that cover the sector of interest S^2. What this means is that there is a change of coordinates so that a "piece" of the unit sphere may be made to look like a finite two-dimensional plane, and vice versa. Hence, in talking about the measurement array A or the unit sphere S^2 we are talking about the same object, up to a nonlinear change of variables, so that all the norms to follow can be made equivalent on either the more easily treated unit sphere S^2 or the true measurement array A. See chapter two of [4] for more information concerning this differential geometry.

We proceed with a characterization of the operator that maps induced magnetic currents on the boundary of the scatterer to the electric scattering amplitude.

Proposition 1. Let $\partial D \subset R^3$ be smooth surface such that $T_{\partial D}$ is defined everywhere, and suppose there are no nontrivial solutions to the interior version of the Stratton-Chu integral equations. Then $F : TL^2(\partial D) \to TL^2(S^2)$ is compact and linear and has dense range in $TL^2(S^2)$.

Proof. Linearity is obvious as $F(g_1 + g_2) = Fg_1 + Fg_2$ for any $g_{1,2}$ in $TL^2(\partial D)$. F is compact, since it has a so-called Hilbert-Schmidt kernel; i.e., $K \in TL^2(ds(\partial D) \times ds(S^2))$. Let $g \in TL^2(\partial D)$ be a magnetic current on ∂D. Let $\hat{\theta}$ and $\hat{\varphi}$ denote the tangential unit vectors on S^2. Then, the previous claim follows, since

$$\|F\|^2_{TL^2(ds(\partial D) \times ds(S^2))} = \int_{S^2} \left| \int_{\partial D} K(\hat{x}, y) ds(y) \right|^2 ds(\hat{x}), \tag{60}$$

$$\leq \frac{k^2}{16\pi^2} \int_{S^2} \int_{\partial D} \left| e^{-ik\langle \hat{x}, y \rangle} \right|^2 ds(\hat{x}), \tag{61}$$

$$\leq \frac{k^2}{16\pi^2} \mu(\partial D) \mu(S^2) < \infty, \tag{62}$$

where $\mu(\partial D)$ and $\mu(S^2)$ are the finite surface measures of the scatterer and the unit sphere, respectively. Now, given that K has a Hilbert-Schmidt kernel, we find that given $g \in TL^2(\partial D)$ a magnetic current on ∂D,

$$\|Fg\|^2_{TL^2(S^2)} \leq \|K\|^2_{TL^2(ds(\partial D) \times ds(S^2))} \|g\|^2_{TL^2(\partial D)} < \infty, \tag{63}$$

proves the image of g is included in $TL^2(S^2)$.

Lastly, we note that our operator F is equivalent up to a $\pi/2$ rotation of the tangential field E_∞ on S^2 with the far-field operator presented in [8] in theorem 7.4, which is known to have dense range in $TL^2(S^2)$, provided that k^2 is not a Dirichlet eigenvalue for the interior problem on ∂D.

We now address the range of the operator F acting on magnetic currents on the surface of the sphere $B_R(c)$ in terms of the restriction of the original operator F to TL^2 current distributions supported on the boundary $B_R(c)$. Below, $F|_{\partial B_R(c)}$ denotes this restriction.

Proposition 2. Let $F|_{\partial B_R(c)}$ be the restriction of F to $B_R(c)$. Then $F|_{\partial B_R(c)}$ possesses a Hilbert adjoint, such that

$$F|^{*}_{\partial B_R(c)} : TL^2(S^2) \to TL^2(\partial B_R(c)) \tag{64}$$

and for $g \in TL^2(S^2)$

$$(F|^{*}_{\partial B_R(c)} g)(y) = -\left(v_{B_R(c)} \wedge \frac{ik}{4\pi}\int_{S^2} e^{ik\langle \hat{x}, y\rangle}\hat{x}\wedge\hat{x}\wedge g(\hat{x})ds(\hat{x})\right)\wedge v_{B_R(c)}, \qquad y \in \partial B_R(c). \tag{65}$$

Proof. Since F is compact and linear between two Hilbert spaces, then by the Riesz representation theorem there exists a bounded linear operator F coinciding with the action of the adjoint F^* of F such that it maps $TL^2(S^2)$ to $TL^2(\partial B_R(c))$. F^* may be computed by equating the pairings

$$\langle Fj, g\rangle_{TL^2(S^2)} = \langle j, F^* g\rangle_{TL^2(\partial B_R(c))} \tag{66}$$

for any $j \in TL^2(\partial B_R(c))$ and $g \in TL^2(S^2)$. Hence, we find that

$$P(j,g) = \langle Fj, g\rangle_{TL^2(S^2)} \tag{67}$$

$$= \int_{S^2}\langle \int_{\partial B_R(c)} e^{-ik\langle \hat{x}, y\rangle}\hat{x}\wedge\hat{x}\wedge j(y)ds(y), \overline{g(\hat{x})}\rangle_{C^2} ds(\hat{x}) \tag{68}$$

$$= \int_{\partial B_R(c)}\langle \int_{S^2} (e^{-ik\langle \hat{x}, y\rangle}\hat{x}\wedge\hat{x}\wedge j(y), \overline{g(\hat{x})})ds(\hat{x})\rangle_{C^2} ds(y) \tag{69}$$

$$= \int_{\partial B_R(c)}\langle j(y), -\left(v_{B_R(c)}\frac{ik}{4\pi}\int_{S^2} e^{-ik\langle \hat{x}, y\rangle}\hat{x}\wedge\hat{x}\wedge g(\hat{x})ds(\hat{x})\right)\wedge v_{B_R(c)}\rangle_{C^2} ds(y) \tag{70}$$

$$= \langle j, F^* g\rangle_{TL^2(\partial B_R(c))}. \tag{71}$$

Hence, the claim is proved.

Next, we address the so-called singular system, or singular value decomposition of F restricted to TL^2 currents on the boundary of the sphere $B_R(c)$. Since F is linear and compact then we know it admits the general representation

$$F|_{\partial B_R(c)} = \sum_{n=1}^{\infty} \sum_{m=-n}^{n} \bigoplus_{j=1}^{2} \sigma_{n,m}^{(j)}(R, c)\varphi_{n,m}^{(j)}(R, c) \otimes \psi_{n,m}^{(j)}(R, c)\,. \tag{72}$$

Here, the superscripts $(j = 1)$ and $(j = 2)$ refer to the tangential components in the $\hat{\theta}$ and $\hat{\phi}$ directions, respectively, and the term $\otimes$ is the tensor or outer product of the two orthonormal bases $\psi_{n,m}^{(j)}$ and $\varphi_{n,m}^{(j)}$ for $j = 1, 2$. We add that the action of $F|_{\partial B_R(c)}$ acting on some TL^2 current j is

$$(F|_{\partial B_R(c)}j)(\hat{x}) = \sum_{n=1}^{\infty} \sum_{m=-n}^{n} \bigoplus_{j=1}^{2} \sigma_{n,m}^{(j)}(R, c)\,\langle j, \varphi_{n,m}^{(j)}(R, c)\rangle \psi_{n,m}^{(j)}\,. \tag{73}$$

We also mention that this decomposition then goes to define the Hilbert adjoint of $F|^{*}_{\partial B_R(c)}$ through

$$F|^{*}_{\partial B_R(c)} = \sum_{n=1}^{\infty} \sum_{m=-n}^{n} \bigoplus_{j=1}^{2} \sigma_{n,m}^{(j)}(R, c)\bar{\varphi}_{n,m}^{(j)} \otimes \bar{\psi}_{n,m}^{(j)}\,, \tag{74}$$

where the above overline denotes complex conjugation. Furthermore, we add that the countable singular system

$$\{\sigma_{n,m}^{A,(j)}, \varphi_{n,m}^{A,(j)}, \psi_{n,m}^{A,(j)}\}_{\{n=1,\, m=-n,\, \ldots,\, n\}}^{\infty}\,, \tag{75}$$

of F: $TL^2(\partial B_R(c)) \to TL^2(A)$ any finite two-dimensional measurement array A may be constructed by determining those functions $\sigma_{n,m}^{A,(j)}$, $\varphi_{n,m}^{A,(j)}$, $\psi_{n,m}^{A,(j)}$ such that any of the following identities are satisfied for $j = 1, 2$.

$$F|_{\partial B_R(c)}\varphi_{n,m}^{A,(j)} = \sigma_{n,m}^{A,(j)}\psi_{n,m}^{A,(j)} \tag{76}$$

$$F|^{*}_{\partial B_R(c)}\psi^{A,(j)}_{n,m} = \sigma^{A,(j)}_{n,m}\varphi^{A,(j)}_{n,m} \tag{77}$$

$$F|_{\partial B_R(c)}F|^{*}_{\partial B_R(c)}\psi^{A,(j)}_{n,m} = (\sigma^{A,(j)}_{n,m})^2\psi^{A,(j)}_{n,m} \tag{78}$$

$$F|^{*}_{\partial B_R(c)}F|_{\partial B_R(c)}\varphi^{A,(j)}_{n,m} = (\sigma^{A,(j)}_{n,m})^2\varphi^{A,(j)}_{n,m}. \tag{79}$$

Solutions of these systems may be computed numerically, with some effort, or determined through the computation of a collection of multidimensional integrals. These integrals stem from the coordinate mapping Ψ from the array A and the segment of the unit sphere S^2 on which we know the scattered field E_∞; i.e., the push forward $\Psi : A \to S^2$ is a diffeomorphism so that the pullback Ψ^{-1} exists and $\Psi^{-1} : S^2 \to A$. In this sense, the measured signal on the two-dimensional array admits the representation

$$E^A_\infty = \sum_{n=1}^{\infty}\sum_{m=-n}^{n}\alpha^m_n\nabla_{S^2}Y^m_n\circ\Psi^{-1} + \beta^m_n\nabla_{S^2}Y^m_n\circ\Psi^{-1}. \tag{80}$$

The next result tells us what the analysis basis for the measured electric scattering amplitude is on A; namely, $\nabla_{S^2}Y^m_n\circ\Psi^{-1}$ and $\nabla_{S^2}Y^m_n\circ\Psi^{-1}$ also provides a more evident formulation of the eigenvalue problem, which must be solved to determine the singular values $\sigma^{A,(1)}_{n,m}$ and $\sigma^{A,(2)}_{n,m}$.

Proposition 3. Let A be a smooth finite two-dimensional manifold with a boundary, such that $\Psi : A \to S^2$ and $\Psi^{-1} : S^2 \to A$ are the usual push forward and pull back mappings. Moreover, let E^A_∞ be the measured electric scattering amplitude on the array A and let $F|_{\partial B_R(c)}$ and $F|^{*}_{\partial B_R(c)}$ denote the restriction of F to $\partial B_R(c)$ and its Hilbert adjoint. Then

$$\psi^{A,(1)}_{n,m} = \nabla_{S^2}Y^m_n\circ\Psi^{-1} \tag{81}$$

$$\psi^{A,(2)}_{n,m} = \hat{x}\wedge\nabla_{S^2}Y^m_n\circ\Psi^{-1}, \tag{82}$$

and $\sigma^{A,(j)}_{n,m}$, $j = 1, 2$ may be determined from

$$F|_{\partial B_R(c)} F|^{*}_{\partial B_R(c)} \nabla_{S^2} Y_n^m \circ \Psi^{-1} = (\sigma_{n,m}^{A,(1)})^2 \nabla_{S^2} Y_n^m \circ \Psi^{-1} \tag{83}$$

$$F|_{\partial B_R(c)} F|^{*}_{\partial B_R(c)} \hat{x} \wedge \nabla_{S^2} Y_n^m \circ \Psi^{-1} = (\sigma_{n,m}^{A,(2)})^2 \hat{x} \wedge \nabla_{S^2} Y_n^m \circ \Psi^{-1}. \tag{84}$$

Proof. Let E_∞^A denote the electric scattering amplitude on the unit sphere S^2 and the array A, respectively, and let j denote the magnetic current giving rise to the two fields. Then,

$$\alpha_{n,m} = \langle E_\infty^A, \nabla_{S^2} Y_n^m \circ \Psi^{-1} \rangle_{L^2(A)} \tag{85}$$

$$= \langle F|_{\partial B_R(c)} j, \nabla_{S^2} Y_n^m \circ \Psi^{-1} \rangle_{L^2(A)} \tag{86}$$

$$= \langle j, \bar{F}|^{*}_{\partial B_R(c)} \nabla_{S^2} Y_n^m \circ \Psi^{-1} \rangle_{L^2(R^3)} \tag{87}$$

$$= \langle j, \sigma_{n,m}^{(1)} \varphi_{n,m}^{A,(1)} \rangle_{L^2(R^3)} \tag{88}$$

$$= \langle P_1 j, \sigma_{n,m}^{A,(1)} \varphi_{n,m}^{A,(1)} \rangle_{L^2(R^3)}. \tag{89}$$

Since $P_1 j$ is the projection of any vector field in $L^2(R^3, C^3)$ onto the orthonormal basis $\{\sigma_{n,m}^{A,(j)}, \varphi_{n,m}^{A,(j)}\}$, this amounts to saying

$$F|^{*}_{\partial B_R(c)} \psi_{n,m}^{A,(1)} = \sigma_{n,m}^{A,(1)} \varphi_{n,m}^{A,(1)} \tag{90}$$

holds for $\psi_{n,m}^{A,(1)} = \nabla_{S^2} Y_n^m \circ \Psi^{-1}$. Similarly, examining the coefficients β_n^m in the much the same way,

$$\beta_{n,m} = \langle E_\infty^A, \hat{x} \wedge \nabla_{S^2} Y_n^m \circ \Psi^{-1} \rangle_{L^2(A)} \tag{91}$$

$$= \langle F|_{\partial B_R(c)} j, \hat{x} \wedge \nabla_{S^2} Y_n^m \circ \Psi^{-1} \rangle_{L^2(A)} \tag{92}$$

$$= \langle j, \bar{F}|^*_{\partial B_R(c)} \hat{x} \wedge \nabla_{S^2} Y_n^m \circ \Psi^{-1} \rangle_{L^2(R^3)} \tag{93}$$

$$= \langle j, \sigma_{n,m}^{A,(2)} \varphi_{n,m}^{A,(2)} \rangle_{L^2(R^3)} \tag{94}$$

$$= \langle P_2\, j, \sigma_{n,m}^{A,(2)} \varphi_{n,m}^{A,(2)} \rangle_{L^2(R^3)}, \tag{95}$$

implies

$$F|^*_{\partial B_R(c)} \psi_{n,m}^{A,(2)} = \sigma_{n,m}^{A,(2)} \varphi_{n,m}^{A,(1)}, \tag{96}$$

and, more precisely, that $\psi_{n,m}^{A,(2)} = \hat{x} \wedge \nabla_{S^2} Y_n^m \circ \Psi^{-1}$. This completes the proof.

The main result presented in this section owes itself in part to what is known as Picard's Theorem. The theorem essentially provides a representation for a compact linear operator A between two Hilbert spaces H_1 and H_2 in terms of the operator's singular system, as well as a means to assess whether a given element of the second space H_2 is also an element of the closure of the range of A. We take a moment to state the theorem and refer to [8] for its proof.

Theorem 3 (Picard). Let $A : H_1 \to H_2$ be a compact linear operator from the Hilbert space H_1 into the Hilbert space H_2 with the denumerable singular system $\{\sigma_n, \phi_n, \psi_n\}_{n=1}^{\infty}$; i.e.,

$$A\phi_n = \sigma_n \psi_n \tag{97}$$

and

$$A^* \psi_n = \sigma_n \phi_n, \tag{98}$$

and let $\langle .,. \rangle$ denote the inner product on H_2. Then, the equation $Af = g$ is solvable if and only if $g \in N(A^*)^{\perp}$ and

$$\sum_{n=1}^{\infty} \frac{|\langle f, \psi_n \rangle|^2}{\sigma_n^2} < \infty . \tag{99}$$

Moreover, any f of the form

$$f = \sum_{n=1}^{\infty} \frac{\langle g, \psi_n \rangle}{\sigma_n} \phi_n , \tag{100}$$

solves $Af = g$.

Finally, we state the following range characterizations of F, which we will need for the proof of the made theorem to follow.

Lemma 1. Let $B_{R_{1,2}}(c_{1,2})$ be of two spheres of radii R_1 and R_2 having centers c_1 and c_2, such that $B_{R_1}(c_1)$ contains $B_{R_2}(c_2)$. Then

$$R(F|_{\partial B_{R_2}(c_2)}) \subset R(F|_{\partial B_{R_1}(c_1)}) . \tag{101}$$

Proof. Let $B_{R_{1,2}}(c_{1,2})$ be as stated above. Let $f_{1,2} \in TL^2(\partial B_{R_{1,2}} c_{(1,2)})$. Then the trivial extension of the form

$$f_1(x) = \begin{cases} f_1(x), & x \in \partial B_{R_1}(c_1) \\ 0, & x \notin \partial B_{R_1}(c_1) \end{cases} \tag{102}$$

proves the claim.

Next, we demonstrate that in the case when the closure of $B_{R_1}(c_1)$ has no intersection with the closure of $B_{R_2}(c_2)$, then the only common element in the ranges of $F|_{\partial B_{R_1}(c_1)}$ and $F|_{\partial B_{R_2}(c_2)}$ is the trivial electric scattering amplitude $E_\infty = 0$. This amounts to saying that two disjoint conducting scatterers can never produce the same electric scattering amplitude on any open set away from their support.

Proposition 4. Let $B_{R_{1,2}}(c_{1,2})$ be as before. Then

$$B_{R_1}(c_1) \cap B_{R_2}(c_2) = \varnothing \iff R(F|_{\partial B_{R_1}(c_1)}) \subset R(F|_{\partial B_{R_2}(c_2)}) = \{0\} . \tag{103}$$

Proof. Each tangential component of E_∞ on S^2 satisfies Rellich's lemma; c.f. [8]. Hence, if we treat each component, this is a immediate consequence of corollary 5.1.2 in [9].

Proof of the Main Theorem. Application of Picard's Theorem to the identified spaces $H_1 = TL^2(\partial B_R(c))$ and $H_2 = TL^2(S^2)$ and the range characterizations of $F|_{\partial B_R(c)}$ now prove the theorem in the previous section. Specifically, Green's theorem proves 1) $\Rightarrow$ 2), while the asymptotics for the generalized Fourier coefficients for any free solution of the Maxwell system on the complement of $B_R(c)$ proves 2) $\Rightarrow$ 3). Lastly, assuming 3) and knowing that the range of $F|_{\partial B_R(c)}$ is dense in $TL^2(S^2)$ and employing lemma 1 and proposition 4 we arrive at 1). (C.f. [9] for the details of these arguments.) This completes the proof.

Given Picard's Theorem, and our range characterization of the operator $F|_{\partial B_R(c)}$, we now have a definitive test that can determine whether a scatterer is fully within some region Ω of interest by means of testing the convergence of the sum

$$\|\tilde{j}\|^2_{TL^2(\partial\Omega)} = \sum_{n=1}^{\infty} \sum_{m=-n}^{n} \left| \frac{\langle E_\infty, \psi^{(1)}_{n,m} \rangle}{\sigma^{(1)}_{n,m}(\Omega)} \right|^2 + \left| \frac{\langle E_\infty, \psi^{(2)}_{n,m} \rangle}{\sigma^{(2)}_{n,m}(\Omega)} \right|^2 . \tag{104}$$

In theory, if the sum does not converge, then we can conclude that the scatterer is not fully within the test region Ω, whereas if the sum does converge, we can conclude that the scattering support of the scatter is fully contained within this set.

We note that this formulation states both Theorems 1 and 2 at the same time; namely, Ω may play the role of the sphere $B_R(c)$ or any other finite multiply connected, possibly nonconvex set. In the more general setting, once we have determined the appropriate singular system for the operator F restricted to the boundary of Ω—i.e., we solve the eigenvalue eigenfunction equations in proposition 3 with $B_R(c)$ simply replaced by the more general Ω—we may perform the same Picard test and conclude whether the scatterer is fully within Ω or not, as indicated by the finiteness of the series. There is good reason to believe that this test may be done in the electromagnetic case discussed here, again on the basis of the numerical procedure and results obtained in [7].

5. SUMMARY AND CONCLUSIONS

The results presented here are fundamental to many advanced radar detection and imaging efforts and offer us an avenue by which the three-dimensional shape of rotating bodies may be determined with narrowband monostatic sensors.

We have rigorously developed and presented the underlying theory of the scattering of a single monochromatic, or narrowband, incident electromagnetic wave and its interaction with a perfectly conducting object. Moreover, we have carefully detailed how this scattering problem leads to a viable and robust reconstruction, or three-dimensional imaging algorithm, that is capable of estimating the size and shape of either a convex or multiply connected nonconvex scatterer with this extremely limited information.

REFERENCES

[1] Kusiak, S., and J. Sylvester. 2003. The scattering support. *Communications on Pure and Applied Mathematics* 56: 1525–48.

[2] Kusiak, S., and J. Sylvester. 2005. The convex scattering support in a background medium. *SIAM Journal on Mathematical Analysis* 36: 1142–58.

[3] Brenner, S.C., and L.R. Scott. 1994. *The mathematical theory of finite elements methods*. New York: Springer-Verlag.

[4] Nédélec, J.-C. 2000. *Acoustic and electromagnetic equations: integral representations for harmonic problems*. New York: Springer-Verlag.

[5] Abramowitz, M., and I.A. Stegun. 1970. *Handbook of mathematical functions*. Washington: National Bureau of Standards, Government Printing Office.

[6] Arfken, G. 1985. *Mathematical methods for physicists*. 3rd ed. Orlando: Academic Press.

[7] Potthast, R., J. Sylvester, and S. Kusiak. 2003. A 'range test' for determining scatterers with unknown physical properties. *Inverse Problems* 19: 533–47.

[8] Colton, D., and R. Kress. 1998. *Inverse acoustic and electromagnetic scattering theory*. 2nd. ed. Berlin: Springer-Verlag.

[9] Kusiak, S. 2003. The scattering support and the inverse scattering problem at fixed frequency. Ph.D. thesis, Dept. of Applied Mathematics, University of Washington.

REPORT DOCUMENTATION PAGE

Form Approved
OMB No. 0704-0188

1. REPORT DATE	2. REPORT TYPE	3. DATES COVERED *(From - To)*
15 February 2008	Technical	

4. TITLE AND SUBTITLE
Advanced Narrowband Electromagnetic Size and Shape Determination

5a. CONTRACT NUMBER
FA8721-05-C-0002

5b. GRANT NUMBER

5c. PROGRAM ELEMENT NUMBER

6. AUTHOR(S)
S. Kusiak

5d. PROJECT NUMBER
342

5e. TASK NUMBER
1

5f. WORK UNIT NUMBER

7. PERFORMING ORGANIZATION NAME(S) AND ADDRESS(ES) AND ADDRESS(ES)

MIT Lincoln Laboratory
244 Wood Street
Lexington, MA 02420-9108

8. PERFORMING ORGANIZATION REPORT NUMBER
TR-1116

9. SPONSORING / MONITORING AGENCY NAME(S) AND ADDRESS(ES)

ADAC—AMP Facility
106 Winn Drive
Huntsville, AL 35801
Attn: T. Lai

10. SPONSOR/MONITOR'S ACRONYM(S)

11. SPONSOR/MONITOR'S REPORT NUMBER(S)
ESC-TR-2006-073

12. DISTRIBUTION / AVAILABILITY STATEMENT
Approved for public release; distribution is unlimited..

13. SUPPLEMENTARY NOTES

14. ABSTRACT

We discuss a fundamental radar imaging problem for narrowband electromagnetic waves that extends the recent results originally obtained in the scalar, or acoustic, setting. In particular we demonstrate the ability to efficiently image three-dimensional convex conducting bodies by using the knowledge of the scattered electric field for one fixed monochromatic illumination of the target. In this problem our knowledge of the scattered electric wave is understood to be in the form of measurements of the amplitude and phase of the tangential components of the radiated electric field (generated by the radar target) on a finite two-dimensional array. We also provide a more general version of this streamlined result that describes imaging of multiply connected nonconvex objects with the same measurements.

15. SUBJECT TERMS

16. SECURITY CLASSIFICATION OF:			17. LIMITATION OF ABSTRACT	18. NUMBER OF PAGES	19a. NAME OF RESPONSIBLE PERSON
a. REPORT	b. ABSTRACT	c. THIS PAGE			19b. TELEPHONE NUMBER *(include area code)*
Unclassified	Unclassified	Unclassified	Same as report	44	